Lithium-Ion Insertion Kinetics of Na-Doped LiFePO$_4$ as Cathode Materials for Lithium-Ion Batteries

YAN-RONG ZHU, RUI ZHANG, LI DENG, TING-FENG YI, MING-FU YE, JIN-HAN YAO, and CHANG-SONG DAI

Na-doped Li$_{1-x}$Na$_x$FePO$_4$ (x = 0, 0.05, 0.1, and 0.2) materials were synthesized by a simple high-temperature solid-state method. The structure, morphology, and kinetic performances of the samples were characterized by X-ray diffraction (XRD), scanning electron microscope (SEM), cyclic voltammetry (CV), and electrochemical impedance spectroscopy (EIS). XRD indicates that all samples are in accordance with the standard LiFePO$_4$ with olivine structure. SEM reveals that the particle size of all samples is about 1 to 2 μm. CV exhibits that Na doping obviously improves the reversibility and dynamic behaviors of lithium intercalation and deintercalation. EIS shows that Na doping decreases the charge transfer resistance of LiFePO$_4$ and improves the lithium diffusion coefficients. It can be concluded that Na doping results in lower electrode polarization and higher lithium-ion diffusion coefficient, which can effectively improve the kinetic performance of LiFePO$_4$.

I. INTRODUCTION

LITHIUM-ION batteries have been considered as one of the most viable candidates for EVs and HEVs because of the highest power and energy density of any existing battery systems.[1,2] Developing positive-electrode materials with high safety is one of the key challenges for lithium-ion batteries. Among the existing cathode chemistries used in lithium batteries, lithium iron phosphate (LiFePO$_4$) offers outstanding power capability, excellent safety characteristics, and low cost compared to Ni- and Co-based layered oxide materials.[3,4] Unfortunately, LiFePO$_4$ suffers from a very low electrical conductivity of about 10^{-9} s cm^{-1} at room temperature,[5,6] so it is difficult to achieve its theoretical capacity when discharged at a high current density. Several approaches have been explored to solve the conductivity problem. These approaches have been carried out including the reduction of particle size,[7,8] surface coatings,[9,10] or aliovalent cation doping.[11–16] The first principles' investigation revealed that LiFePO$_4$ is most affected by F ion doping at O site with the narrowest band gap, followed by Mn ion doping at Fe site and Na ion doping at Li site, indicating that appropriate ion doping in LiFePO$_4$ could improve its electronic conductivity.[17,18]

Solid-state synthesis is a conventional method to prepare electrode material and exhibits a potential commercial application due to the simple synthesis route and low synthesis cost.[19,20] The chemical diffusion coefficient of lithium ion (D_{Li}) is one of the most important kinetic characteristics of an electrochemical intercalation process in electrode materials.[21,22] The determining step of rate in the electrodes of lithium ion batteries is supposed to be the solid-state diffusion.[23] Hence, D_{Li} plays a very important role in the study of electrodes materials for lithium-ion batteries. Many relevant techniques have been proposed for the evaluation of D_{Li}, *e.g.*, the capacity, potentiostatic, and galvanostatic intermittent titration technique (CITT, PITT, and GITT, respectively)[24–26] and electrochemical impedance spectroscopy (EIS).[27,28] EIS has been considered as a very powerful technology to determine the rate of individual electrode kinetic steps because it can also be obtained under more equilibrium conditions compared with other methods. In addition, the low-frequency Warburg of EIS is directly related to the lithium-ion diffusion process in an electrode material.[29]

In the paper, olivine Li$_{1-x}$Na$_x$FePO$_4$(x = 0, 0.05, 0.1 and 0.2) is successfully synthesized by a solid-state method, and the structure and kinetic properties are evaluated.

YAN-RONG ZHU, Experimentalist, RUI ZHANG and LI DENG, Undergraduate Students, TING-FENG YI, Professor, and MING-FU YE, Lecturer, are with the School of Chemistry and Chemical Engineering, Anhui University of Technology, Maanshan, Anhui 243002, P.R. China. Contact e-mail: tfyihit@163.com and yemingfu@ahut.edu.cn JIN-HAN YAO, Associate Professor, is with the State Key Laboratory Breeding Base of Green Chemistry-Synthesis Technology, College of Chemical Engineering and Material Science, Zhejiang University of Technology, Hangzhou, Zhejiang 310014, P.R. China. Contact e-mail: jhyao@zjut.edu.cn CHANG-SONG DAI, Professor, is with the School of Chemical Engineering and Technology, Harbin Institute of Technology, Harbin, Heilongjiang 150001, P.R. China.
Manuscript submitted September 2, 2014.
Article published online January 8, 2015.

II. EXPERIMENTAL

Analytical reagents of FeC$_2$O$_4$·2H$_2$O, NH$_4$H$_2$PO$_4$, Na$_2$CO$_3$, and Li$_2$CO$_3$ were used for this work. The Li$_{1-x}$Na$_x$FePO$_4$(x = 0, 0.05, 0.1 and 0.2) composite was synthesized via a solid-state reaction. The stoichiometric proportion reagents mentioned above were

placed in an agate bowl. The mixtures were ball milled in 20 mL ethanol at a rotating speed of about 200 rpm for 5 to 6 hours. After the ethanol was removed, the precursor mixture was pre-heat treated at 623 K (350 °C) for 5 hours and then 973 K (700 °C) for 10 hours under a nitrogen atmosphere. The samples were naturally cooled to room temperature.

The X-ray diffractometry (XRD) measurements were performed on a Rigaku instrument with Cu Kα radiation. Scanning electron microscopy (SEM) was performed to observe the particles morphology. Cyclic voltammetry (CV) test was carried out on a CHI-852C electrochemical workstation with a voltage between 2.5 and 4.3 V at a scanning rate of 0.1 mV/s. Electrochemical impedance spectroscopy (EIS) is measured by a CHI 760D (Shanghai Chenhua, China) electrochemical working station over a frequency range from 0.01 Hz to 10 kHz at a potentiostatic signal amplitude of 5 mV. The prepared electrode materials were adopted as the working electrode; the counter electrode and reference electrode were Li foil.

A CR2025 coin-cell assembly was used for the electrochemical characterization. Slurry was formed by mixing the $Li_{1-x}Na_xFePO_4$ (80 pct), acetylene black (10 pct), and binder (10 wt pct polyvinylidene fluoride, dissolved in N-methyl-2-pyrrolidone). The slurry was coated onto the aluminum foil from which pellets of 14 mm in diameter were cut as electrodes. The half-cells were assembled with a composite cathode and a metallic lithium anode separated by porous polypropylene film (Celgard 2300) filled with 1 m $LiPF_6$ in ethylene carbonate/dimethyl carbonate (1:1 by vol.) solution.

III. RESULTS AND DISCUSSION

Figure 1 shows the XRD patterns of $Li_{1-x}Na_xFePO_4$ (x = 0, 0.05, 0.1, and 0.2) samples. It can be found that the XRD patterns of the Na-doped samples are similar to that of the standard orthorhombic $LiFePO_4$. The crystal phases of all the samples are ordered olivine
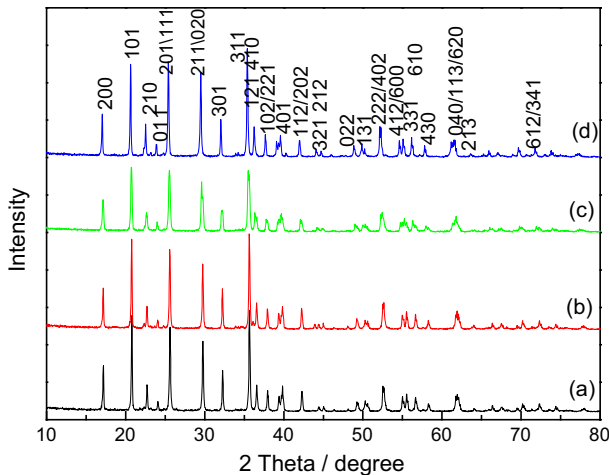
structure indexed orthorhombic Pnma, and no extra reflection is observed. It is obvious that Na doping does not affect the structure of the samples, and Na^+ probably enters into the lattice of $LiFePO_4$ rather than form impurities.

Figure 2 gives the enlarged XRD patterns of the peak (101) for $Li_{1-x}Na_xFePO_4$ (x = 0, 0.05, 0.1, and 0.2) samples. It can be found that the samples with the Na doping undergo a slight shift toward lower degrees. Since there were no peaks of impurity, and the positions of the main diffraction peaks after Na doping shift lower angle compared with the standard $LiFePO_4$, it may be concluded that Na was inserted the internal lattice and caused an increase in interplanar distance. According to the previous report, the doping of Na ion would be inclined to occupy Li sites because the phase of $NaFePO_4$ was structurally analogous to $LiFePO_4$[30,31] and that Na and Li atoms have the same outer electronic structure.[32] Na^+ serves as a pillar in the structure, which can stabilize the crystal structure.[32] The reason without impurity peaks may be that a partial solid solution of $LiFePO_4$-$NaFePO_4$ when the doped content of Na is high. The corresponding lattice parameters of $Li_{1-x}Na_xFePO_4$ obtained from XRD are listed in Table I.

With incorporation of Na^+ ions, the cell volume becomes larger. However, we note that the elementary cell volume of $Li_{1-x}Na_xFePO_4$ is slightly less than for $NaFePO_4$ olivine structure (V = 312.6 $Å^3$) as the ionic volume of Na^+ is almost twice that of Li^+.[33] The
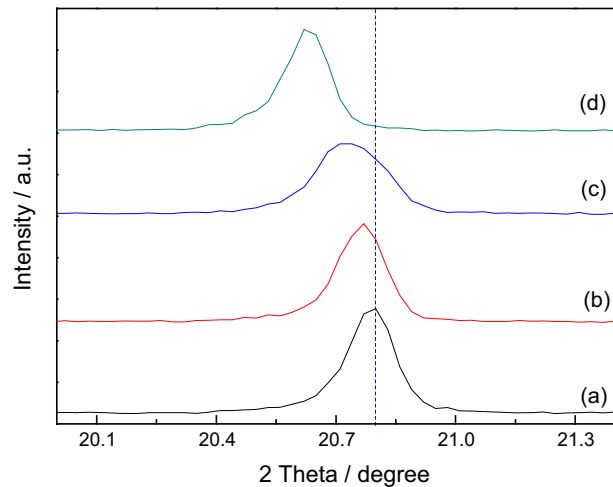

Fig. 2—Enlarged (101) peak of XRD patterns for $Li_{1-x}Na_xFePO_4$ powder (a) x = 0, (b) x = 0.05, (c) x = 0.1, and (d) x = 0.2.

Fig. 1—XRD patterns of $Li_{1-x}Na_xFePO_4$ powder (a) x = 0, (b) x = 0.05, (c) x = 0.1, and (d) x = 0.2.

Table I. Lattice Parameters of $Li_{1-x}Na_xFePO_4$

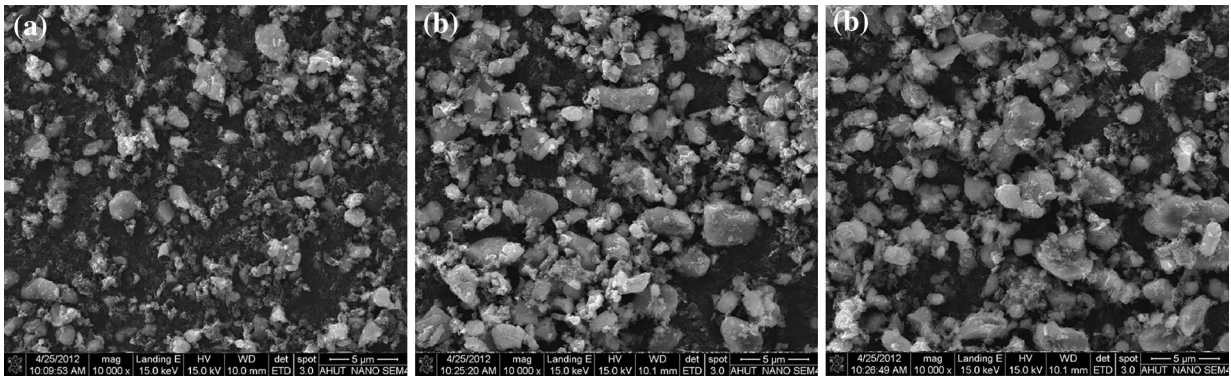| Sample	a (Å)	b (Å)	c (Å)	V (Å^3)
$LiFePO_4$	10.294	6.009	4.712	291.468
$Li_{0.95}Na_{0.05}FePO_4$	10.310	6.015	4.721	292.771
$Li_{0.9}Na_{0.1}FePO_4$	10.316	6.023	4.728	293.767
$Li_{0.8}Na_{0.2}FePO_4$	10.322	6.035	4.736	295.021

Fig. 3—SEM images of the as-prepared $Li_{1-x}Na_xFePO_4$ (*a*) *x* = 0, (*b*) *x* = 0.05, (*c*) *x* = 0.1.
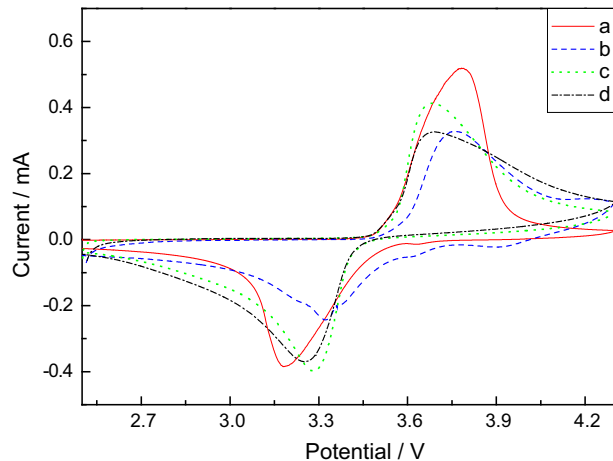
Fig. 4—Cyclic voltammetry curves of the $Li_{1-x}Na_xFePO_4$ materials (*a*) *x* = 0, (*b*) *x* = 0.05, (*c*) *x* = 0.1, and (*d*) *x* = 0.2.

increasing of the lattice parameter can enhance the Li^+ intercalation/deintercalation.[34] This result is attributed to the larger ionic radii of Na^+ (1.02 Å[35]) compared with that of Li^+ (0.76 Å[35]). It has been reported that Li^+ ion migration of $LiFePO_4$ occurs preferentially via one-dimensional channels oriented along the [010] direction of the orthorhombic crystal structure due to the smallest lithium migration energy along the [010] one-dimensional tunnel with the continuous chain of edge-shearing LiO_6 octahedra.[14] Hence, it can be concluded that the doping of Na can enlarge the interplanar distance of (101) crystal plane. This means that Na doping increases the Li ion pathway in [010] direction.[36]

SEM images of the pristine and doped $LiFePO_4$ samples are shown in Figure 3. It can be seen that all samples are composed of irregular particles, and the particle sizes of the three samples are almost in the same range of 1 to 2 μm. The irregular particles may be due to the solid-state synthesis. Apparently, doping with Na^+ does not change the morphology of $LiFePO_4$. However, some agglomeration of $LiFePO_4$ solid powders can be found. From this point of view, the particle size effect on the lithium-ion insertion kinetics of the samples may be ruled out, and the dissimilarity of the samples, in term of

kinetic performance, can mainly be attributed to the Na-substitution.

Figure 4 shows the cyclic voltammograms of $Li_{1-x}Na_xFePO_4$ (*x* = 0, 0.05, 0.1, and 0.2) samples measured at a sweep rate 0.1 mV s^{-1} in the first cycle. It is obviously that a single pair of sharp oxidation and reduction peaks, ascribing to the two-phase reaction of the Fe^{3+}/Fe^{2+} redox couple, can be clearly discerned. The peaks parameters of the various samples from the CV plots are listed in Table II.

The potential differences between anodic and cathodic peaks reflect the polarization degree of the electrode. For pristine $LiFePO_4$, the oxidation and reduction peaks occur at 3.797 and 3.182 V, respectively, with the potential difference being 615 mV. Obviously, the potential separations between the anodic and cathodic peaks for the Na-doped $LiFePO_4$ samples are lower than those of $LiFePO_4$. It indicates that Na doping is beneficial to the reversible intercalation and deintercalation of Li^+, so it enhances the reversibility of the $LiFePO_4$.[37] Especially, the oxidation and reduction peaks of $Li_{0.9}Na_{0.1}FePO_4$ are located at 3.688 and 3.283 V, respectively, and the potential difference is 405 mV. It has been reported that a broadened peak of pristine $LiFePO_4$ means poor kinetics, sluggish lithium intercalation, and deintercalation. However, a sharp peak of $LiFePO_4$ highlights excellent kinetics and facile lithium intercalation and deintercalation.[38] This indicates that Na-doped $LiFePO_4$ has lower electrochemical polarization and more excellent kinetics than that of pristine $LiFePO_4$. The lower polarization and excellent kinetics of Na-doped $LiFePO_4$ samples can be attributed to the higher electronic conductivity improved by Na doping compared with that of $LiFePO_4$.

In order to further study the effect of Na doping on the kinetics process of the electrode materials, electrochemical impedance spectroscopy (EIS) measurement of $Li_{1-x}Na_xFePO_4$ (*x* = 0, 0.05, 0.1, and 0.2) was carried out in the frequency range between 10 kHz and 0.1 Hz, which is shown in Figure 5. The inset shows the selected equivalent circuit used to fit the EIS and the enlarged Nyquist plots of the $Li_{1-x}Na_xFePO_4$ materials for *x* = 0.05 and *x* = 0.1. All curves show one compressed semicircle in the medium-frequency region and an inclined line in the low-frequency range.

Table II. Parameters of the CV Peaks and EIS for $Li_{1-x}Na_xFePO_4$ (x = 0, 0.05, 0.1, 0.2)

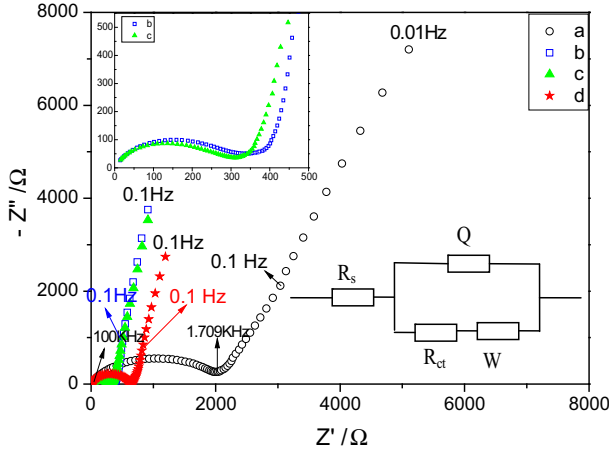| Samples	E_{pa} (V)	E_{pc} (V)	E_p (mV)	R_s/Ω	R_{ct}/Ω
$LiFePO_4$	3.797	3.182	615	13.34	1650
$Li_{0.95}Na_{0.05}FePO_4$	3.761	3.322	439	3.839	229.1
$Li_{0.9}Na_{0.1}FePO_4$	3.688	3.283	405	4.129	254.4
$Li_{0.8}Na_{0.2}FePO_4$	3.692	3.251	441	4.369	537.3

Fig. 5—Nyquist plots of the $Li_{1-x}Na_xFePO_4$ materials (*a*) x = 0, (*b*) x = 0.05, (*c*) x = 0.1, and (*d*) x = 0.2 (Note: Inset is the selected equivalent circuit used to fit the EIS).

The high-frequency semicircle always corresponds to the charge transfer process (R_{ct}),[39,40] and the fitted R_{ct} data are listed in Table II. It was found the overall charge transfer resistance of the Na-doped electrodes decreased gradually with the increase of Na concentration ($x \leq 0.1$), and it was much smaller than that of the pristine $LiFePO_4$. $Li_{0.9}Na_{0.1}FePO_4$ exhibits the smallest charge transfer resistance among all samples, suggesting that $Li_{0.9}Na_{0.1}FePO_4$ may have the highest electrochemical activity during cycling. The R_s reflects electric conductivity of the electrolyte, separator, and electrodes, and the fitted R_s data are listed in Table II.

It can be found that the R_s values of the Na-doped electrodes are much smaller than that of the pristine $LiFePO_4$, indicating that Na-doping electrodes exhibit much smaller solution than the pristine $LiFePO_4$. In the low-frequency region, the sloping line of Na-doped $LiFePO_4$ is larger than pristine $LiFePO_4$, revealing that the Na-doped $LiFePO_4$ are more favorable for the intercalation/deintercalation of lithium ions into/from the bulk solid phase.[41] This indicates that Na doping can enhance the electronic conductivity of $LiFePO_4$. The straight line with a slope in low-frequency region is attributed to the diffusion of the lithium ions into the bulk of the electrode material or the so-called Warburg diffusion.[42,43] The lithium-ion diffusion coefficient (D_{Li}) can be calculated from the plots in the low-frequency region according to the following equations (Eqs. [1] and [2])[44–52]—similar approach has also been applied in various cathode materials like $LiFePO_4$,[46–48] $LiNi_{0.5}Mn_{1.5}O_4$,[49] LiV_3O_8,[50] $LiMn_2SiO_4$,[51] and $Li_4Ti_5O_{12}$[52] electrode materials:

Fig. 6—(*a*) Graph of Z_{re} plotted against $\omega^{-1/2}$ at low-frequency region for $Li_{1-x}Na_xFePO_4$ electrodes for x = 0, x = 0.05, x = 0.1, and x = 0.2; (*b*) the enlarged graph of Z_{re} plotted against $\omega^{-1/2}$ of the $Li_{1-x}Na_xFePO_4$ materials for x = 0.05 and x = 0.1.

$$D_{Li} = \frac{R^2 T^2}{2 A^2 n^4 F^4 C_{Li}^2 \sigma^2}, \qquad [1]$$

$$Z_{re} = R_{ct} + R_s + \sigma \omega^{-\frac{1}{2}}, \qquad [2]$$

where T is the absolute temperature; R is the gas constant; A is the surface area of the electrode; F is the Faraday constant; n is the number of electrons per molecule during oxidation; C_{Li} is the concentration of lithium ion; and σ is the Warburg factor which is related to Z_{re} obtained from the slope of the lines in Figure 6. The selected low-frequency region ranges from 0.01 to 0.1 Hz.
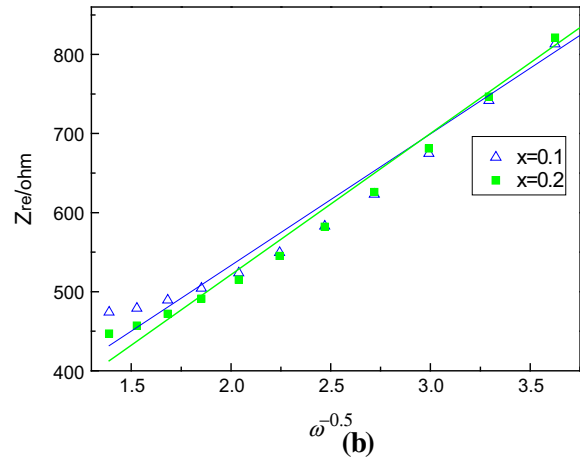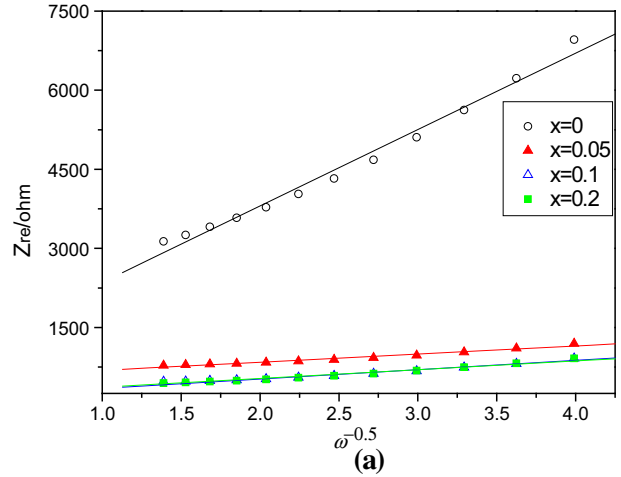
The diffusion coefficient values of $Li_{1-x}Na_xFePO_4$ (x = 0, 0.05, 0.1 and 0.2) are 1.21×10^{-16}, 1.06×10^{-14}, 7.95×10^{-15}, and 9.17×10^{-15} cm^2 s^{-1}, respectively. It is obvious that the lithium diffusion coefficients increase due to the Na doping. This result clearly indicates that the lithium-ion mobility of $LiFePO_4$ can be effectively improved by moderate Na doping. The reason maybe is that the Na doping increases the Li ion pathway in [010] direction.

IV. CONCLUSIONS

$Li_{1-x}Na_xFePO_4$ (x = 0, 0.05, 0.1, and 0.2) powders were successfully synthesized by a simple high-temperature solid-state method. Na ions have successfully been doped into the $LiFePO_4$ phase, and the particle size of all samples is around 1 to 2 μm. The low potential interval demonstrates that the lithium insertions into the Na-doped $LiFePO_4$ electrodes can be treated as a quasi-reversible system with improved dynamic behaviors. Na doping can not only reduce the charge transfer resistance but also increase the diffusion coefficient of lithium ion. Therefore, the Na doping is an effective approach to achieve excellent kinetic performance for the $LiFePO_4$ positive-electrode materials.

REFERENCES

1. J. Yang, X.-Y. Zhou, Y.-L. Zou, and J.-J. Tang: *Electrochim. Acta*, 2011, vol. 56, pp. 8576–81.
2. M. Masih-Tehrani, M.-R. Ha'iri-Yazdi, V. Esfahanian, and A. Safaei: *J. Power Sour.*, 2013, vol. 244, pp. 2–10.
3. L. Dimesso, C. Förster, W. Jaegermann, J.P. Khanderi, H. Tempel, A. Popp, J. Engstler, J.J. Schneider, A. Sarapulova, D. Mikhailova, L.A. Schmitt, S. Oswald, and H. Ehrenberg: *Chem. Soc. Rev.*, 2012, vol. 41, pp. 5068–80.
4. N. Alias and A.A. Mohamad: *J. Power Sour.*, 2015, vol. 274, pp. 237–51.
5. J. Lee, P. Kumar, J. Lee, B.M. Moudgil, and R.K. Singh: *J. Alloys Compd.*, 2013, vol. 550, pp. 536–44.
6. H.-J. Kim, J.-M. Kim, W.-S. Kim, H.-J. Koo, D.-S. Bae, and H.-S. Kim: *J. Alloys Compd.*, 2011, vol. 509, pp. 5662–66.
7. J. Mun, H.-W. Ha, and W. Choi: *J. Power Sour.*, 2014, vol. 251, pp. 386–92.
8. E. Hosono, Y. Wang, N. Kida, M. Enomoto, N. Kojima, M. Okubo, H. Matsuda, Y. Saito, T. Kudo, I. Honma, and H. Zhou: *ACS Appl. Mater. Interfaces*, 2010, vol. 2, pp. 212–18.
9. T. Kozawa, N. Kataoka, A. Kondo, E. Nakamura, H. Abe, and M. Naito: *Ceram. Int.*, 2014, vol. 40, pp. 16127–31.
10. D. Ziolkowska, K.P. Korona, B. Hamankiewicz, S.-H. Wu, M.-S. Chen, J.B. Jasinski, M. Kaminska, and A. Czerwinski: *Electrochim. Acta*, 2013, vol. 108, pp. 532–39.
11. R. Trócoli, S. Franger, M. Cruz, J. Morales, and J. Santos-Peña: *Electrochim. Acta*, 2014, vol. 135, pp. 558–67.
12. A.Y. Shenouda and H.K. Liu: *J. Alloys Compd.*, 2009, vol. 477, pp. 498–503.
13. K.L. Harrison, C.A. Bridges, M.P. Paranthaman, C.U. Segre, J. Katsoudas, V.A. Maroni, J.C. Idrobo, J.B. Goodenough, and A. Manthiram: *Chem. Mater.*, 2013, vol. 25, pp. 768–81.
14. M.S. Islam, D.J. Driscoll, C.A.J. Fisher, and P.R. Slater: *Chem. Mater.*, 2005, vol. 17, pp. 5085–92.
15. T. Honma, K. Nagamine, and T. Komatsu: *Ceram. Int.*, 2010, vol. 36, pp. 1137–41.
16. I. Bilecka, A. Hintennach, M.D. Rossell, D. Xie, P. Novák, and M. Niederberger: *J. Mater. Chem.*, 2011, vol. 21, pp. 5881–90.
17. J. Xu and G. Chen: *Physica B*, 2010, vol. 405, pp. 803–07.
18. M. Milović, D. Jugović, N. Cvjetićanin, D. Uskoković, A.S. Milošević, Z.S. Popović, and F.R. Vukajlović: *J. Power Sour.*, 2013, vol. 241, pp. 70–79.
19. D. Jugović and D. Uskoković: *J. Power Sour.*, 2009, vol. 190, pp. 538–44.
20. J.W. Fergus: *J. Power Sour.*, 2010, vol. 195, pp. 939–54.
21. F. Lantelme, A. Mantoux, H. Groult, and D. Lincot: *Solid State Ionics*, 2006, vol. 177, pp. 205–09.
22. H. Manjunatha, T.V. Venkatesha, and G.S. Suresh: *Electrochim. Acta*, 2011, vol. 58, pp. 247–57.
23. X.H. Rui, N. Ding, J. Liu, C. Li, and C.H. Chen: *Electrochim. Acta*, 2010, vol. 55, pp. 2384–90.
24. H. Manjunatha, K.C. Mahesh, G.S. Suresh, and T.V. Venkatesha: *Electrochim. Acta*, 2012, vol. 80, pp. 269–81.
25. C. Montella: *Electrochim. Acta*, 2006, vol. 51, pp. 2778–81.
26. D.W. Dees, S. Kawauchi, D.P. Abraham, and J. Prakash: *J. Power Sour.*, 2009, vol. 189, pp. 263–68.
27. M. Talebi-Esfandarani and O. Savadogo: *Solid State Ionics*, 2014, vol. 261, pp. 81–86.
28. K. Tang, X. Yu, J. Sun, H. Li, and X. Huang: *Electrochim. Acta*, 2011, vol. 56, pp. 4869–75.
29. T.-F. Yi, Y. Xie, Q. Wu, H. Liu, L. Jiang, M. Ye, and R. Zhu: *J. Power Sour.*, 2012, vol. 214, pp. 220–26.
30. J.N. Birdson, S.E. Quinlan, and P.R. Tremaine: *Chem. Mater.*, 1998, vol. 10, pp. 763–68.
31. V. Palomares, P. Serras, I. Villaluenga, K.B. Hueso, J. Carretero-González, and T. Rojo: *Energy Environ. Sci.*, 2012, vol. 5, pp. 5884–5901.
32. Z.H. Wang, L.X. Yuan, M. Wu, D. Sun, and Y.H. Huang: *Electrochim. Acta*, 2011, vol. 56, pp. 8477–83.
33. K. Zaghib, J. Trottier, P. Hovington, F. Brochu, A. Guerfi, A. Mauger, and C.M. Julien: *J. Power Sour.*, 2011, vol. 196, pp. 9612–17.
34. Z. Ma, G. Shao, G. Wang, Y. Zhang, and J. Du: *J. Solid State Chem.*, 2014, vol. 210, pp. 232–37.
35. R.D. Shannon: *Acta Crystallogr.*, 1976, vol. A3, pp. 751–67.
36. D. Morgan, A.V. der Ven, and G. Ceder: *Electrochem. Solid State Lett.*, 2004, vol. 7, pp. A30–A32.
37. C. Gong, Z. Xue, X. Wang, X.-P. Zhou, X.-L. Xie, and Y.-W. Mai: *J. Power Sour.*, 2014, vol. 246, pp. 260–68.
38. G. Qin, Q. Wu, J. Zhao, Q. Ma, and C. Wang: *J. Power Sour.*, 2014, vol. 248, pp. 588–95.
39. M.M. Rahman, J.-Z. Wang, R. Zeng, D. Wexler, and H.K. Liu: *J. Power Sour.*, 2012, vol. 206, pp. 259–66.
40. K. Bazzi, B.P. Mandal, M. Nazri, V.M. Naik, V.K. Garg, A.C. Oliveira, P.P. Vaishnava, G.A. Nazri, and R. Naik: *J. Power Sour.*, 2014, vol. 265, pp. 67–74.
41. C. Miao, P. Bai, Q. Jiang, S. Sun, and X. Wang: *J. Power Sour.*, 2014, vol. 246, pp. 232–38.
42. O. Toprakci, H.A.K. Toprakci, L. Ji, G. Xu, Z. Lin, and X. Zhang: *ACS Appl. Mater. Interfaces*, 2012, vol. 4, pp. 1273–80.
43. L. Wang, Z. Li, H. Xu, and K. Zhang: *J. Phys. Chem. C*, 2008, vol. 112, pp. 308–12.
44. M. Vujković, I. Stojković, N. Cvjetićanin, and S. Mentus: *Electrochim. Acta*, 2013, vol. 92, pp. 248–56.

45. N. Takami, A. Satoh, M. Hara, and T. Ohsaki: *J. Electrochem. Soc.*, 1995, vol. 142, pp. 371–79.
46. H. Liu, Q. Cao, L.J. Fu, C. Li, Y.P. Wu, and H.Q. Wu: *Electrochem. Commun.*, 2006, vol. 8, pp. 1553–57.
47. X. Qin, X. Wang, J. Xie, and L. Wen: *J. Mater. Chem.*, 2011, vol. 21, pp. 12444–48.
48. Y. Zhou, J. Wang, Y. Hu, R. O'Hayre, and Z. Shao: *Chem. Commun.*, 2010, vol. 46, pp. 7151–53.
49. J. Wang, W. Lin, B. Wu, and J. Zhao: *Electrochim. Acta*, 2014, vol. 145, pp. 245–53.
50. S. Sarkar, H. Banda, and S. Mitra: *Electrochim. Acta*, 2013, vol. 99, pp. 242–52.
51. S. Liu, J. Xu, D. Li, Y. Hu, X. Liu, and K. Xie: *J. Power Sour.*, 2013, vol. 232, pp. 258–63.
52. B. Li, C. Han, Y.B. He, C. Yang, H. Du, Q.H. Yang, and F. Kang: *Energy Environ. Sci.*, 2012, vol. 5, pp. 9595–9602.